Head and Neck Pathology (2020) 14:554–558
https://doi.org/10.1007/s12105-019-01055-9

CASE REPORT

New Insights into Tumor Heterogeneity: A Case of Solid-Oncocytic Epithelial-Myoepithelial Carcinoma of the Parotid Gland Harboring a *HRAS* and Heterogeneous Terminating *ARID1A* Mutation

Niels J. Rupp[1,5] · Muriel Brada[1,5] · Alena Skálová[2] · Beata Bode[1,3,5] · Martina A. Broglie[4,5] · Grégoire B. Morand[4,5] · Markus Rechsteiner[1,5] · Sandra N. Freiberger[1,5]

Received: 2 June 2019 / Accepted: 10 July 2019 / Published online: 15 July 2019

Abstract
Epithelial-myoepithelial carcinoma (EMC) can be a challenging diagnosis due to a lack of obvious invasion and bland cytology. We report an unusual case of a low-grade EMC with prominent fibrous stroma, an extensive solid-oncocytic differentiation and limited areas of morphological clearly identifiable characteristic biphasic (tubular) differentiation, clear cells and PAS-positive secretions/calcifications. Both areas were investigated by next generation sequencing (Oncomine comprehensive assay) and revealed a typical concordant *HRAS* p.Q61R mutation. An additional heterogeneous *ARID1A* (p.E672*) terminating mutation with loss of heterozygosity, which could be visualized predominantly in the solid-oncocytic differentiation by immunohistochemical loss of ARID1A protein expression, was found. This is the first case of an EMC of the salivary gland to be described with two separate tumor clones involving concordant *HRAS* and heterogeneous *ARID1A* mutations. The latter seem to be a "second hit" and was predominantly found in the solid-oncocytic differentiation, suggesting a potential morpho-molecular association.

Keywords Epithelial myoepithelial carcinoma · Salivary gland · Solid · Oncocytic · Heterogeneous · ARID1A · HRAS

Introduction

Salivary gland epithelial-myoepithelial carcinoma (EMC) is a low-grade tumor characterized by a typical biphasic epithelial-myoepithelial growth pattern, clear myoepithelial differentiated abluminal cells and intraluminal secretions [1, 2]. EMC is in most cases lobulated, well circumscribed and/or encapsulated mimicking a benign lesion including (cellular) pleomorphic adenoma, whereas EMC ex pleomorphic adenoma (ex PA) can also be observed [1, 3]. Recently, morphological variants such as oncocytic (-sebaceous), apocrine and double-clear have been described, extending the morphological spectrum of EMC [4, 5]. Rarely, high-grade transformation, also known as "dedifferentiation", can be observed in a minority of EMC cases, characterized by necrosis, anaplasia and/or myoepithelial overgrowth [3]. On a molecular level, recurrent *HRAS* mutations can be found in EMC, and *PLAG1/HMGA2* translocations in EMC ex PA [3, 6]. Here, we describe an unusual case of an overwhelmingly solid-oncocytic differentiated EMC in the parotid gland of a 70-year-old female patient, with two tumor clones, both harboring a comprehensive *HRAS* p.Q61R mutation and a heterozygous loss of *ARID1A*, while only one of the clones presented with a hitherto, in this entity unpublished, *ARID1A* terminating mutation.

✉ Niels J. Rupp
niels.rupp@usz.ch

1 Department of Pathology and Molecular Pathology, University Hospital Zurich, Schmelzbergstr. 12, 8091 Zurich, Switzerland

2 Sikl's Department of Pathology, Faculty of Medicine in Plzen, Charles University, Pilsen, Czech Republic

3 Institute of Pathology Enge, Zurich, Switzerland

4 Department of Otorhinolaryngology, Head and Neck Surgery, University Hospital Zurich, Zurich, Switzerland

5 University of Zurich, Zurich, Switzerland

Case Report

Clinical Presentation

A 70-year-old female was referred to our Department of Otorhinolaryngology—Head and Neck Surgery for a painless nodule at the angle of the left mandible for a few months. Clinical exam revealed a mobile firm mass in the deep parotid. Facial nerve function was symmetrical. Ultrasound showed a hypoechoic well-circumscribed round mass of up to 1.95 cm in diameter inside the parotid gland, directly posterior to the mandible. No enlarged or suspicious lymph nodes were detected by MRI and ultrasound of the neck.

Cytology

The ultrasound-guided fine needle aspiration showed a cellular salivary gland neoplasm with an epithelial/myoepithelial differentiation and discreet atypia. Differential diagnosis encompassed basal cell adenoma, cellular pleomorphic adenoma and low-grade salivary gland carcinoma including epithelial-myoepithelial carcinoma.

Resection Specimen Morphology

The nodule was arising from the deep parotid lobe. It was resected completely without sacrifice/injury to any branches of the facial nerve. The postoperative period was uneventful showing symmetrical facial nerve function. The resection specimen was submitted entirely and formalin-fixed, paraffin-embedded. Tissue was examined on 2 µm-thick hematoxylin & eosin (H&E) stained sections. The H&E morphology showed a very well circumscribed and encapsulated, lobulated cellular salivary gland neoplasm (Fig. 1a) with sectional obvious biphasic epithelial-myoepithelial differentiation, including minimal cleared myoepithelial cells, intraluminal secretions and some calcifications (Fig. 1b). Focal prominent fibrous stroma was noted (Fig. 1c). Besides, overwhelming solid-oncocytic differentiation was evident, in which a biphasic growth pattern was more difficult to appreciate (Fig. 1d). Some mitotic figures were visible. Focal infiltration into the capsule and intravascular tumor complexes could be noted (Fig. 1e), but no convincing extension beyond the capsule. No perineural infiltration or areas of a pleomorphic adenoma were apparent.

Resection Specimen Immunohistochemistry

The overall biphasic population of epithelial and myoepithelial cells could be corroborated by positive staining for p63 (abluminal myoepithelial cells) and CD117 (luminal epithelial cells) in both compartments (Fig. 1d insets, Table 1). Virtually all tumor cells showed diffuse nuclear positivity for SOX10 in both cell types (epithelial and myoepithelial cells), and all areas. No nuclear expression of PLAG1 or β-Catenin was present. MIB-1 proliferation index was worrisome at around 10–15%. A typical

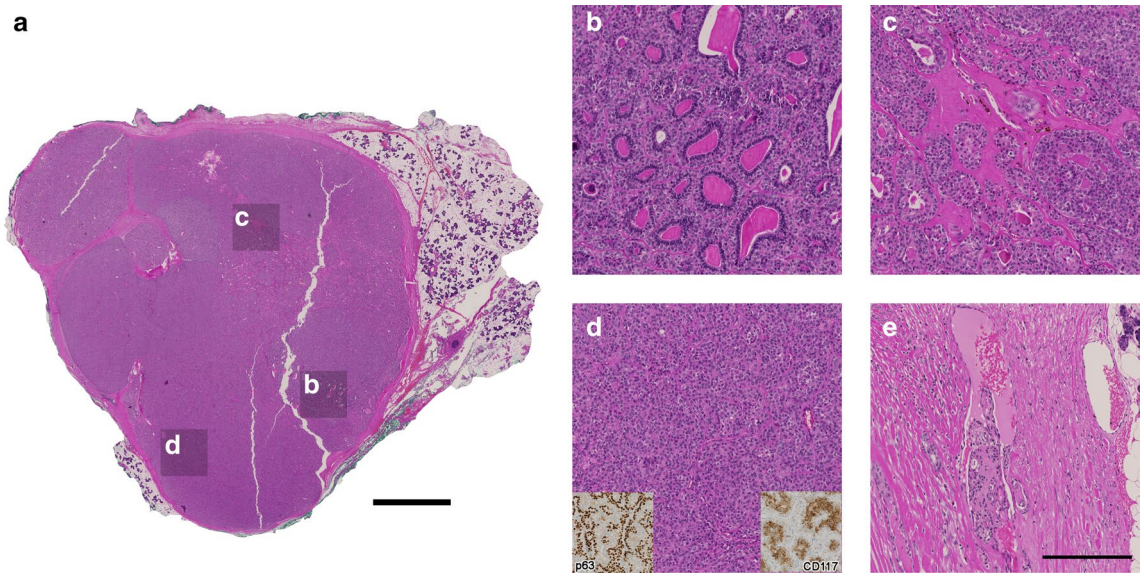

Fig. 1 Overview of this epithelial-myoepithelial carcinoma. **a** Shows the lobulated and encapsulated cellular neoplasm. In **b** a more typical epithelial-myoepithelial differentiation is seen with cystic epithelial structures filled with secretions and focal calcifications. **c** Depicts the focal prominent fibrous stroma dissecting the epithelial cells, whereas **d** shows the more solid-oncocytic differentiation, corroborated by p63 and CD117 staining (insets) visualizing the biphasic, epithelial-myoepithelial differentiation. In **e** intravascular tumor complexes are visible in the capsule region, being surrounded by endothelium (different slide as shown in (**a**). Scale bar 2.5 mm (**a**) and 250 µm (**b**–**e**)

Table 1 Overview of the immunohistochemical stainings performed

Immunohistochemistry	Result
PLAG1	Negative
CD117	Positive in epithelial component
P63	Positive in myoepithelial component
SOX10	Positive in both components
S100	Positive, predominantly in epithelial component
Nuclear β-Catenin	Negative
MIB-1	10–15%
ARID1A	One clone preserved expression (tubular component), one clone loss of expression (more solid-oncocytic component)

wild-type pattern of p53 staining was found. Staining for ARID1A protein showed two distinct tumor clones, whereas the expression was especially lost in the solid-oncocytic differentiated areas and preserved in the more classical, tubular areas (Fig. 2).

Molecular Testing Using Next Generation Sequencing

Next generation sequencing (NGS) using the Oncomine comprehensive assay v3 (LifeTechnologies) revealed a *HRAS* p.Q61R mutation in both investigated areas. Furthermore, both areas had a heterozygous loss of *ARID1A*. Additionally, a terminating *ARID1A* mutation (p. E672*)

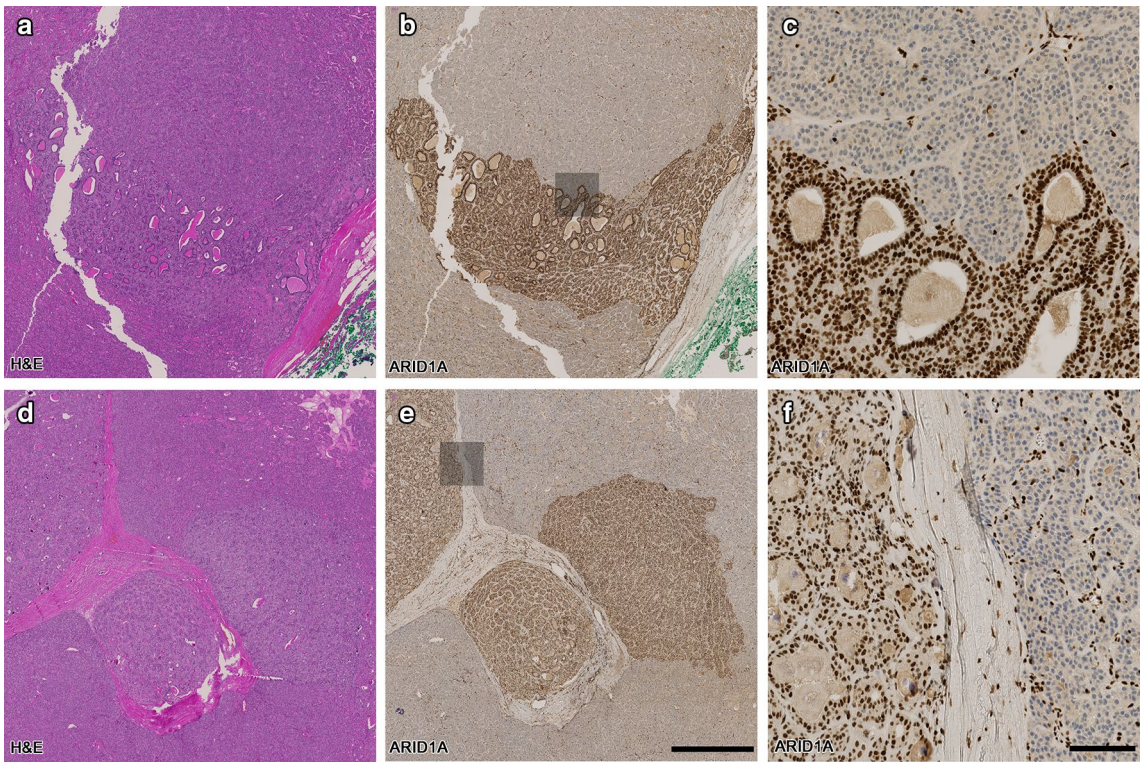

Fig. 2 Morphological overview of different tumor clones in this epithelial-myoepithelial carcinoma. **a** Shows more classical region with cystic glandular structures containing prominent secretions in the lower right corner. **b** Shows preserved expression of ARID1A in this region, whereas the adjacent solid-oncocytic differentiation demonstrates total loss of ARID1A expression. In **c** a magnification of the separating line between the two clones can be appreciated. Similarly, **d** shows another region with lightening morphology in a central and right beside nodule, as well as more tubular differentiation in the left upper corner. These nodules show strong expression of ARID1A (**e**), whereas the adjacent darker regions have lost the expression. In **f** a magnification of the two tumor clones can be seen with prominent secretions in the ARID1A conserved clone on the left. Scale bar 1 mm (**a**–**b**, **d**–**e**); scale bar 100 µm (**c**, **f**)

was found in the solid differentiated areas while *ARID1A* was wildtype in a more classical tubular area, corresponding to loss of expression and expression in the ARID1A immunohistochemistry, respectively. No fusions of *PLAG1*- or *HMGA2* were found using the Archer FusionPlex Sarcoma panel (ArcherDx).

Finally, diagnosis of low-grade EMC with solid-oncocytic differentiation was provided, corroborated by the typical described *HRAS* p.Q61R mutation. Interestingly, the terminating *ARID1A* mutation was found only in one tumor clone, whereas the other clone was *ARID1A* wildtype in the molecular testing. These results correlated well with the expression pattern of ARID1A protein by immunohistochemistry.

The tumor was resected completely with negative surgical margins. The histology was discussed at the local interdisciplinary head & neck tumor board with decision that no adjuvant treatment was required. No follow up data are available because the case was recent.

Discussion

We report the first case of a heterogeneous *ARID1A* mutation with loss of heterozygosity in addition to a typical *HRAS* p.Q61R mutation in a salivary gland EMC. So far, *HRAS* mutations were found in around 30% of EMC in the literature [3, 6], whereas a very recent study reported *HRAS* mutations in up to 82.7% of EMC in a large cohort including different morphologic subtypes [7]. Furthermore, cases with isolated *PLAG1* or *HMGA2* translocations have been described, typically encountered in cases with EMC ex PA [3]. Rarely, EMC shows high-grade transformation/dedifferentiation, whereas in a larger study by El Hallani et al. additional aberrations in *TP53*, *FBXW7* and *SMARCB1* were found [3]. In breast adenomyoepitheliomas, which are morphologically related to EMC, similar findings with *HMGA2* translocations, activating *HRAS* mutations or mutations in *PIK3CA* and *AKT1* were described recently [8, 9]. The AT-rich interactive domain-containing protein 1A (ARID1A) encoded by the *ARID1A* gene is part of the SWI/SNF chromatin remodeling complex and has a tumor-suppressing function [10]. *ARID1A* mutations have been very well characterized in ovarian clear cell carcinoma and endometrioid adenocarcinoma [11], whereas aberrations in *ARID1A* have been described only very rarely in salivary gland tumors: a *ARID1A-PRKD1* fusion has been reported in cribriform adenocarcinoma of salivary gland origin by Weinreb et al. [12]. Moreover, Sebastiao et al. recently showed a terminating p.Q288Pfs*71 frameshift *ARID1A* deletion in a polymorphous adenocarcinoma [13]. Terminating mutations and frameshift mutations leading to early termination of ARID1A protein translation and thereby to a loss of function, have been described previously in salivary gland carcinomas (12/114 sequenced salivary gland tumors) encompassing in addition salivary duct carcinoma (2/18 samples) and adenoid cystic carcinoma (10/73 samples) [14]. However, none of these samples showed a heterozygous deletion of *ARID1A* in addition. *ARID1A* mutations are known in various types of cancer, whereas they can affect either one or both alleles, e.g. in ovarian clear-cell carcinomas [15]. While some of the tumors retain protein expression, most of them are lacking it, suggesting haploinsufficiency of *ARID1A*. The EMC of our patient showed two different morphologies. While the *HRAS* mutation was most likely the driver in both of them, loss of heterozygosity of *ARID1A* tumor suppressor acted as a probable second hit and was predominantly found in the more solid-oncocytic than the more classical tubular growth pattern. In vitro and in vivo studies had shown anti-tumor activities of several targeted inhibitors, such as ATR-, PARP- or AKT inhibitors [16–18]. These findings have recently led to clinical trials that investigate the effectiveness of several targeted monotherapies or combinational therapies, including combinations with immunotherapy (NCT03718091, NCT02286687, NCT03682289, NCT02576444, NCT03842228, NCT03297424), in solid tumors.

Conclusion

Epithelial-myoepithelial carcinoma with solid-oncocytic differentiation may harbor besides *HRAS* mutations additional *ARID1A* terminating mutations. The loss of ARID1A expression in one tumor clone may be a "second hit" and suggests a morpho-molecular association, as it was mainly found in the solid-oncocytic differentiation. Additional studies of this rare entity are needed to further assess these considerations.

Compliance with ethical standards

Conflict of interest The authors declare that no competing financial interests exist.

Ethical approval The patient provided a written informed consent in accordance with the Declaration of Helsinki.

References

1. Seethala RR, Barnes EL, Hunt JL. Epithelial-myoepithelial carcinoma: a review of the clinicopathologic spectrum and immunophenotypic characteristics in 61 tumors of the salivary glands and upper aerodigestive tract. Am J Surg Pathol. 2007;31(1):44–57. https://doi.org/10.1097/01.pas.0000213314.74423.d8.
2. Yang GC, Soslow RA. Epithelial-myoepithelial carcinoma of the parotid. A case of ductal-predominant presentation with

cytologic, histologic and ultrastructural correlations. Acta Cytol. 1999;43(6):1113–8. https://doi.org/10.1159/000331363.
3. El Hallani S, Udager AM, Bell D, Fonseca I, Thompson LDR, Assaad A, et al. Epithelial-myoepithelial carcinoma: frequent morphologic and molecular evidence of preexisting pleomorphic adenoma, common HRAS mutations in PLAG1-intact and HMGA2-intact cases, and occasional TP53, FBXW7, and SMARCB1 alterations in high-grade cases. Am J Surg Pathol. 2018;42(1):18–27. https://doi.org/10.1097/PAS.0000000000000933.
4. Seethala RR, Richmond JA, Hoschar AP, Barnes EL. New variants of epithelial-myoepithelial carcinoma: oncocytic-sebaceous and apocrine. Arch Pathol Lab Med. 2009;133(6):950–9. https://doi.org/10.1043/1543-2165-133.6.950.
5. Seethala RR. Oncocytic and apocrine epithelial myoepithelial carcinoma: novel variants of a challenging tumor. Head Neck Pathol. 2013;7(Suppl 1):S77–84. https://doi.org/10.1007/s12105-013-0461-0.
6. Chiosea SI, Miller M, Seethala RR. HRAS mutations in epithelial-myoepithelial carcinoma. Head Neck Pathol. 2014;8(2):146–50. https://doi.org/10.1007/s12105-013-0506-4.
7. Urano M, Nakaguro M, Yamamoto Y, Hirai H, Tanigawa M, Saigusa N, et al. Diagnostic significance of HRAS mutations in epithelial-myoepithelial carcinomas exhibiting a broad histopathologic spectrum. Am J Surg Pathol. 2019. https://doi.org/10.1097/PAS.0000000000001258.
8. Geyer FC, Li A, Papanastasiou AD, Smith A, Selenica P, Burke KA, et al. Recurrent hotspot mutations in HRAS Q61 and PI3 K-AKT pathway genes as drivers of breast adenomyoepitheliomas. Nat Commun. 2018;9(1):1816. https://doi.org/10.1038/s41467-018-04128-5.
9. Pareja F, Geyer FC, Brown DN, Sebastiao APM, Gularte-Merida R, Li A, et al. Assessment of HMGA2 and PLAG1 rearrangements in breast adenomyoepitheliomas. NPJ Breast Cancer. 2019;5:6. https://doi.org/10.1038/s41523-018-0101-7.
10. Wu JN, Roberts CW. ARID1A mutations in cancer: another epigenetic tumor suppressor? Cancer Discov. 2013;3(1):35–43. https://doi.org/10.1158/2159-8290.CD-12-0361.
11. Wiegand KC, Shah SP, Al-Agha OM, Zhao Y, Tse K, Zeng T, et al. ARID1A mutations in endometriosis-associated ovarian carcinomas. N Engl J Med. 2010;363(16):1532–43. https://doi.org/10.1056/NEJMoa1008433.
12. Weinreb I, Zhang L, Tirunagari LM, Sung YS, Chen CL, Perez-Ordonez B, et al. Novel PRKD gene rearrangements and variant fusions in cribriform adenocarcinoma of salivary gland origin. Genes Chromosomes Cancer. 2014;53(10):845–56. https://doi.org/10.1002/gcc.22195.
13. Sebastiao APM, Pareja F, Kumar R, Brown DN, Silveira C, da Silva EM, et al. Genomic analysis of recurrences and high-grade forms of polymorphous adenocarcinomas. Histopathology. 2019. https://doi.org/10.1111/his.13854.
14. Zehir A, Benayed R, Shah RH, Syed A, Middha S, Kim HR, et al. Mutational landscape of metastatic cancer revealed from prospective clinical sequencing of 10,000 patients. Nat Med. 2017;23(6):703–13. https://doi.org/10.1038/nm.4333.
15. Jones S, Wang TL, Shih Ie M, Mao TL, Nakayama K, Roden R, et al. Frequent mutations of chromatin remodeling gene ARID1A in ovarian clear cell carcinoma. Science. 2010;330(6001):228–31. https://doi.org/10.1126/science.1196333.
16. Williamson CT, Miller R, Pemberton HN, Jones SE, Campbell J, Konde A, et al. ATR inhibitors as a synthetic lethal therapy for tumours deficient in ARID1A. Nat Commun. 2016;7:13837. https://doi.org/10.1038/ncomms13837.
17. Shen J, Peng Y, Wei L, Zhang W, Yang L, Lan L, et al. ARID1A deficiency impairs the DNA damage checkpoint and sensitizes cells to PARP inhibitors. Cancer Discov. 2015;5(7):752–67. https://doi.org/10.1158/2159-8290.CD-14-0849.
18. Samartzis EP, Gutsche K, Dedes KJ, Fink D, Stucki M, Imesch P. Loss of ARID1A expression sensitizes cancer cells to PI3 K- and AKT-inhibition. Oncotarget. 2014;5(14):5295–303. https://doi.org/10.18632/oncotarget.2092.